16th ICAAR LISBOA 2020-2022

16th International Conference on
Alkali-Aggregate Reaction in Concrete
Lisboa | LNEC | Portugal | 31 May - 2 June 2022

http://icaar2020-2022.lnec.pt

Structural stability assessment of concrete hydraulic structures affected by AAR

Mahdi Ben Ftima [(1)], Maxime Bolduc [(2)], Pierre Léger [(3)]

(1) Polytechnique Montréal, Canada, mahdi.ben-ftima@polymtl.ca

(2) IDAE Consulting Engineers, Montréal, Canada, maxime.bolduc@idae.ca

(3) Polytechnique Montréal, Canada, pierre.leger@polymtl.ca

Abstract

Adequate structural safety margin must be demonstrated while performing stability assessment of alkali-aggregate reaction (AAR) affected gravity dams, gated spillways water intake structures and powerhouses. To this end, several AAR concrete constitutive models are proposed in the literature and implemented in different finite element (FE) computational platforms. For a confident use, the related computer programs should be subjected to a formal verification and validation process. Herein, the AAR FE analysis of a typical hydroelectric facility is performed with a multi-physics AAR model implemented in ABAQUS to identify potential failure modes (PFMs). Comparisons between displacement versus load control siding responses are first presented. Then, three benchmark problems are developed following a top-down approach to assess the capability of AAR FE models to characterize key PFMs in complement to other benchmark problems available in the literature. Those are related to (1) excessive compressive stresses, leading to crushing of thin spillway bridge components, (2) flexural failure at the base of spillway piers due to perpendicular AAR thrust of an adjacent gravity dam, and (3) cracking at the base of concrete walls connected obliquely with each other.

***Keywords**: alkali-aggregate reaction; benchmark problems; finite element model; hydroelectric facility; structural stability*

1. INTRODUCTION

Structural stability, functionality and durability of hydraulic concrete structures are significantly affected by concrete swelling due to alkali-aggregate reaction (AAR). Anisotropic volumetric concrete swelling results in imposed differential displacements on structural components leading to the (1) appearance of micro and macro cracks, or zones with large compressive and shear stresses, (2) disturbance in the equilibrium of internal forces, and (3) distortion of mechanical equipment (Fig.1.1). An effective management of hydroelectric facilities affected by AAR requires the use of finite element technology with dedicated AAR concrete constitutive models [1,2]. Those are used in combination with comprehensive in-situ monitoring and material testing programs to obtain data for their calibration. The key objectives of AAR FE models are therefore to assist (1) in performing a diagnostic to explain the causes of observable displacements and degraded conditions, (2) to establish a prognostic for the transient evolution of AAR that can lead to unacceptable states of functionality, stability and related potential failure modes (PFMs), (3) in developing effective corrective actions, if need be.

AAR FE models have been proposed in the literature with different sophistication degrees to represent the multi-physic processes involved in estimating concrete swelling: (1) reaction kinetics, (2) internal and external restraints to free swelling, (3) temperature, and (4) humidity [3,4]. The development of reliable AAR FE models must follow a rigorous verification and validation (V&V) process to quantify the accuracy of the numerical results. According to [5] "*Verification is the process of assessing software correctness and numerical accuracy of the solution to a given mathematical model. Validation is the process of assessing the physical accuracy of a mathematical model based on comparisons between computational* results *and experimental data".* Series of benchmark AAR problems have been proposed for V&V of AAR constitutive models in [6,7]. Those were developed following a "*bottom-up*" approach starting with unit testing at the material level, then progressing towards structural components and the complete system (Fig.1.2). At the other end of the spectrum, ICOLD committee on numerical analysis of dams conducted benchmark of whole concrete dams affected by AAR (e.g. Kariba arch dam [8]).

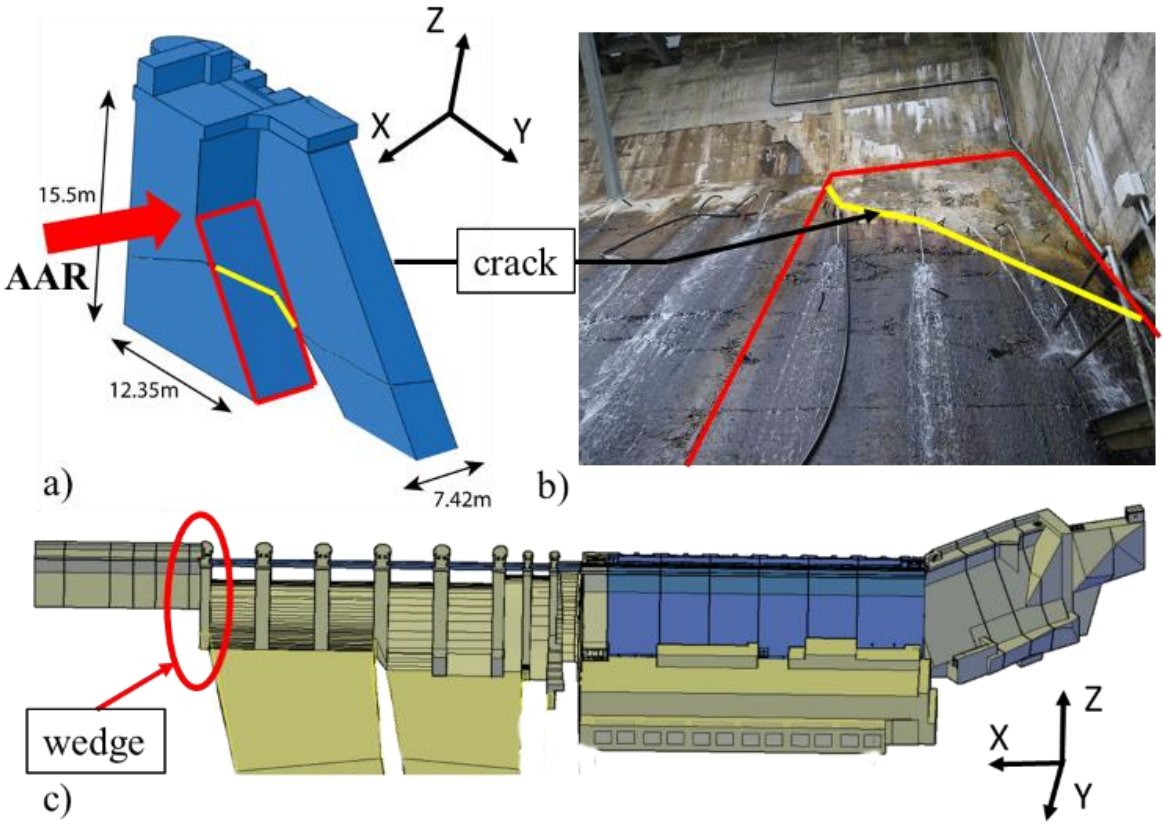

Figure 1.1: Hydroelectric facility affected by AAR, (a) spillway pier, (b) observed crack, (c) formation of a concrete wedge.

Herein, we propose three new and complementary simple benchmark problems derived from a *"top-down approach*" for the verification of AAR models. The AAR FE analysis of the typical hydroelectric facility at the top of the pyramid (Fig. 1.2a) was performed to identify PFMs (Fig.1.3). Relevant benchmark problems (BPs) to verify the capability of AAR models to characterize these PFMs have then been developed. First, the sliding safety assessment of a simplified 3D block structure is presented to highlight differences between force driven and AAR displacement driven sliding stability problems**.** Then, BP1 assesses the capability to model compressive failure (crushing) for certain geometric configurations where small concrete elements are acting in series with larger and stiffer concrete elements (FM No.2 in Fig.1.3). BP2 addresses the case where AAR thrust (displacement driven effects) are combined with hydrostatic pressures (load driven effects) leading to flexural failure of a pier (FM No.1 in Fig 3). Finally, BP3 represents a typical problem occurring at a corner junction between two hydroelectric facility concrete components (FM No.5 in Fig.1.3).

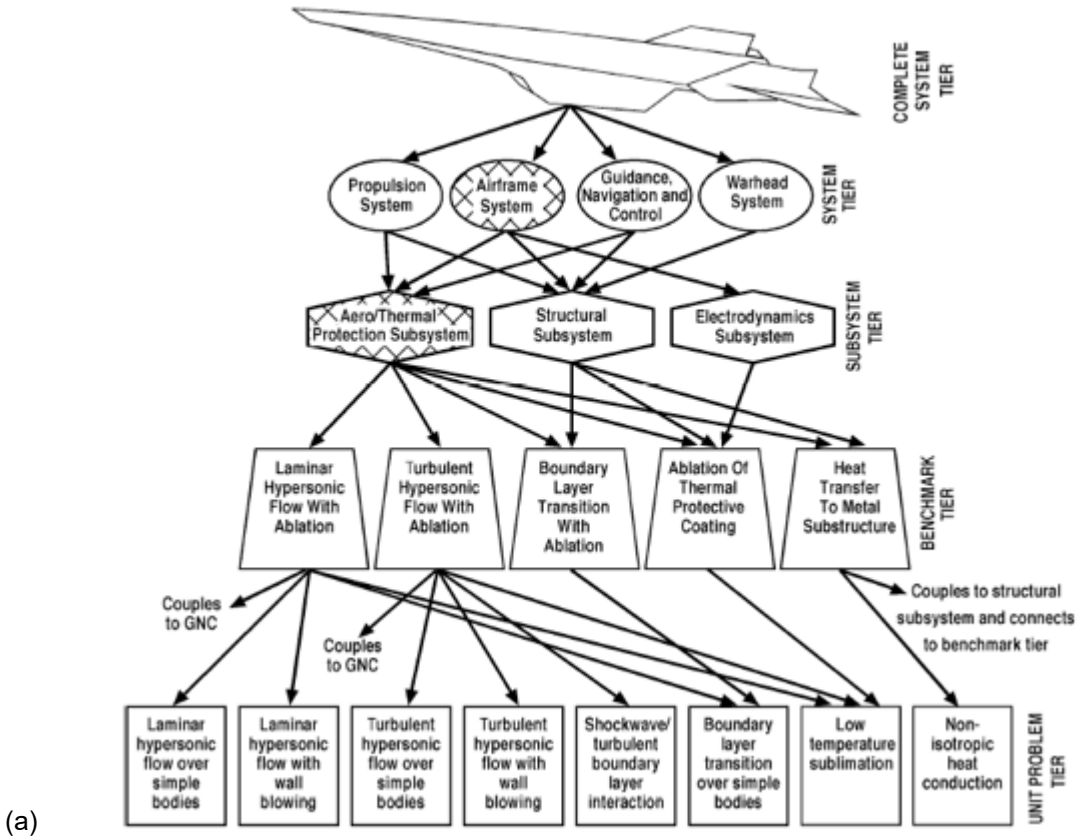

(a)

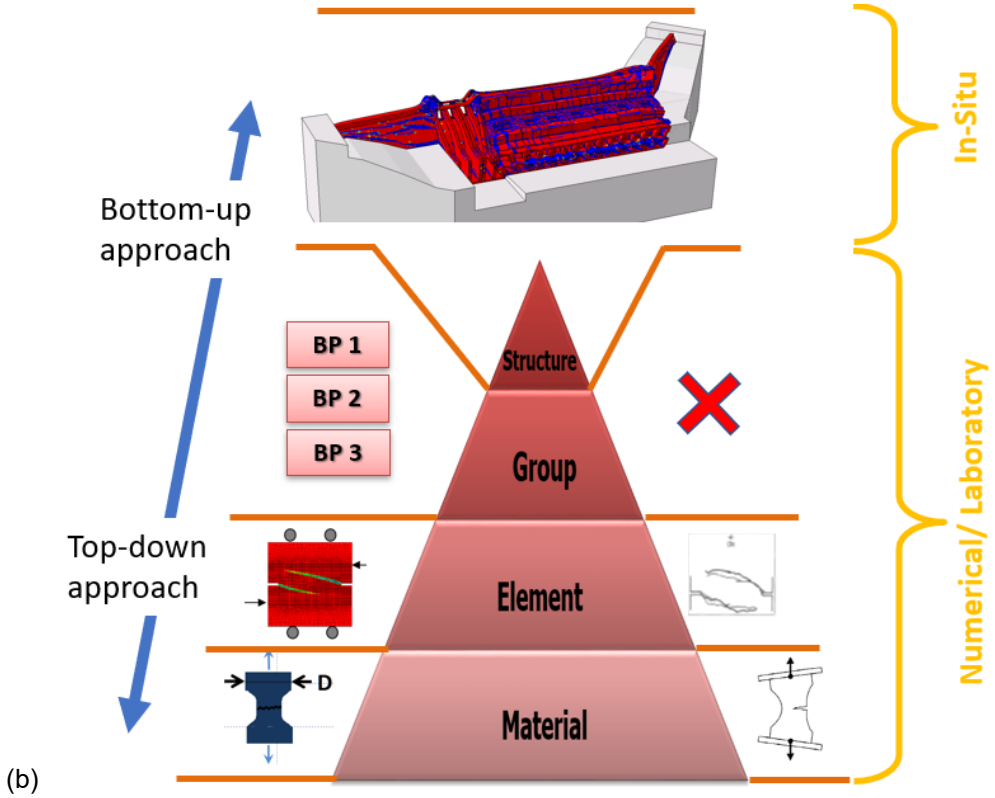

(b)

Figure 1.2: Verification and Validation process (a) in aerospace industry [5], (b) in AAR structural engineering

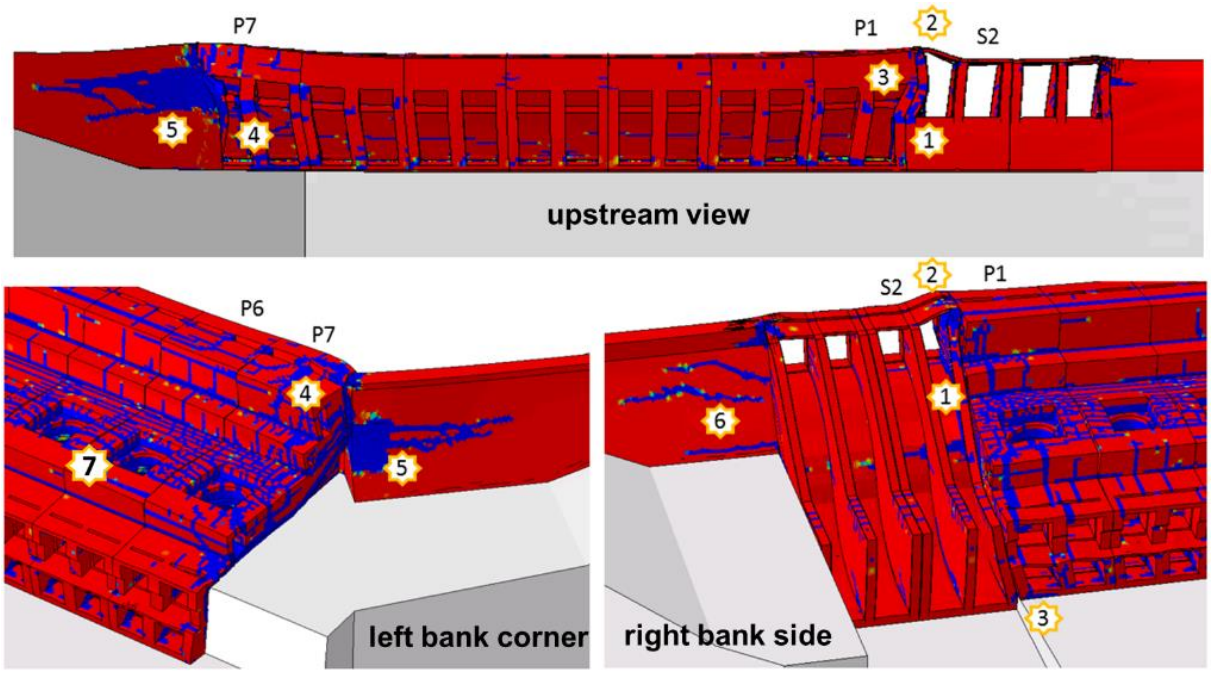

Figure 1.3: Potential Failures Modes (PFMs No.1-7) for AAR affected hydroelectric facilities ($\mathbf{P_i}$ identifies the water intake unit No.; $\mathbf{S_i}$ identify the spillway gate unit No.

2. AAR FE MODELLING AND SIMULATIONS

The AAR FE model used herein has been adapted from Saouma [7] and implemented in the computer program ABAQUS-EXPLICIT by Ben Ftima et al. [9]. A proper modeling and simulation of the AAR kinetic is an essential component to make plausible predictions (extrapolations), that are outside of the timeframe of available monitoring data used for model calibration (Fig. 2.1). Of major interest is the potential for residual expansion at any given time. The AAR simulations for all BP presented below have been performed using the so called "Larive" kinetic model [7,10] with input parameters indicated in Fig 2.1, for a 100 yrs total duration to characterise PFMs. The mechanical input parameters for the concrete constitutive model are given in Table 2.1. A relatively higher bound value is used for the compressive stress σ_u above which swelling will stop [7,13] and a lower bound value is used for the tensile strength f_t' of concrete. At this stage, we did not introduce an inhrent transient reduction of concrete elastic modulus, compressive strength and tensile strength due to swelling progress. There is no consideration for creep (or relaxation). Of course, more elaborate assumptions could be progressively introduced to consider inherent material degradation and creep.

The coupling between the stress field and AAR kinetics follows Saouma model [7]. A retardation of AAR due to compressive and tensile microcracks (Γ_c and Γ_t coefficients in [7]) is considered on the volumetric AAR strain increment. Additionally, weights coefficients (W_i in [7]) are used to distribute volumetric strain along each direction *i*, depending on confinement conditions.

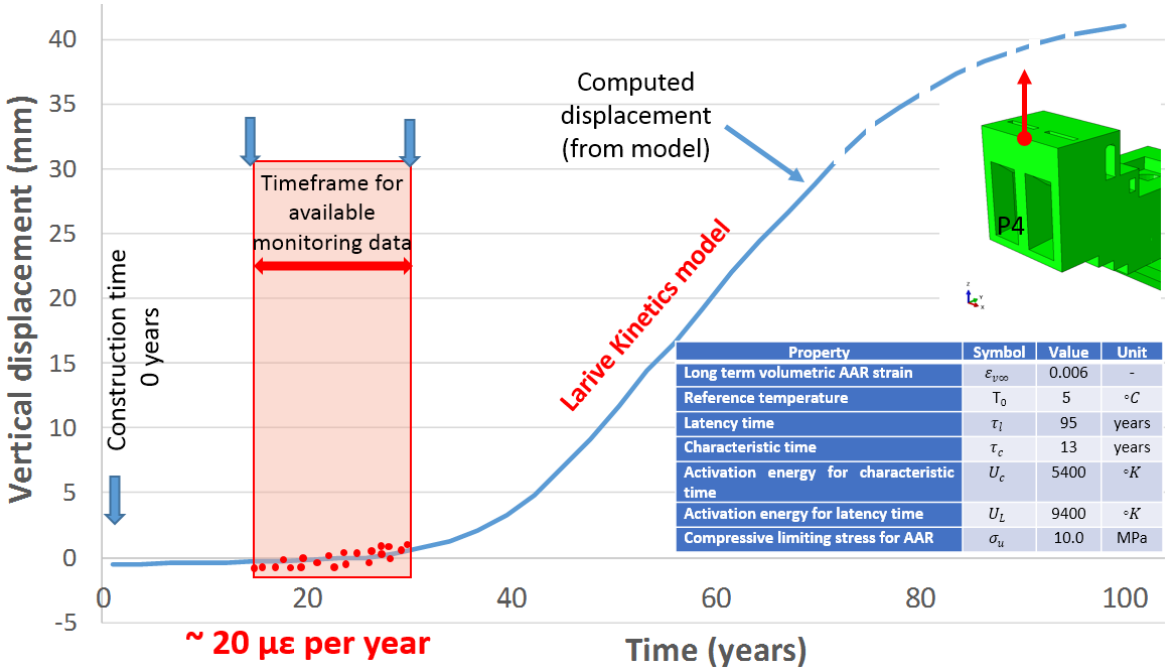

Figure 2.1: AAR kinetic model use in Finite Element simulations

Table 2.1: Mechanical input parameters used in all BPs

Property	Symbol	Value	Unit
Mass density of concrete	ρ	2 400	kg/m^3
Young modulus of concrete	E	27 500	MPa
Compressive strength of concrete	f_c'	40.0 for BP1 30.0 for BP2&3	MPa
Compressive stress stopping swelling	σ_u	10	MPa
Tensile strength of concrete	f_t'	1.8	MPa
Yield strength of reinforcement	f_y	400	MPa
Young modulus of reinforcement	E_s	200 000	MPa
Poisson's ratio of concrete	ν	0.18	-
Mode I fracture energy of concrete	G_F	0.15	kN/m
Young modulus of rock	E	50 000	MPa
Poisson's ratio of rock	ν	0.25	-

3. DISPLACEMENT VERSUS LOAD DRIVEN FAILURE MODES

3.1 Failure modes

Adequate structural safety margins must be demonstrated while performing serviceability and stability assessment of the hydroelectric facilities comprising (i) gravity wing dams, (ii) gated spillways, (iii) water intake structures, and (iv) powerhouse for usual, unusual and extreme (flood, earthquake) conditions.

Figure 1.3 illustrates the PFMs of these components after 100 years of AAR swelling under usual operating conditions. Those are [11]:

(1) Flexural failure or coupled flexural/shear failure of spillway piers under the thrust from the intake upper blocks;
(2) Brittle shear/crushing failure of the bridge supporting structure above the spillway upstream part of hydraulic passage;
(3) Flexural failure or coupled flexural/shear failure of the right-side wall of P1 (intake + draft tube walls);
(4) Flexural failure or coupled flexural/shear failure of the left-side wall of P7 (only intake walls, as draft tube walls in this case are supported by rock);
(5) Wedge stability of the block of left wing dam above the inclined crack;
(6) Wedge stability of the block of right wing dam above the inclined crack;
(7) Tensile yielding of vertical reinforcement of semi-spiral case walls, due to the formation of horizontal or sub-horizontal cracks and corresponding residual tensile stresses;
(8) All other local or global PFMs that may initiate in planes of weakness induced by critical cracks (e.g. inclined shear cracks along the hydraulic passage that cut the powerhouse unit in two blocks requiring strength assessment along this plane).

Three BP have been developed in section 4 to address PFMs No. 1, 2, and 5 described above.

3.2 Displacement driven sliding response

Before tackling PFMs, it is useful to make a clear distinction between (1) load control failure (e.g. excessive hydrostatic thrust), and (2) imposed AAR displacement driven failure. Concrete cracking is a brittle mode, with a sudden release of the corresponding tensile force. Sliding is more of a ductile nature where the mobilized shear strength, or the resisting force, **R**, is maintained when sliding motion is taking place. AAR produces imposed structural displacements which are limited to a few tens, or even a few hundred, millimeters at most. On the other hand, AAR can for example induce small movements (cracks) along the concrete-rock interface, lift joints, or in bulk concrete. This might then reduce shear resistance from peak to residual values. Uplift pressures may increase in cracks and joints. Excessive hydrostatic thrust, a load driven mode, is then likely to set a structural element in motion leading to structural instability of detached concrete blocks characterized by unbounded displacements [12].

Figure 3.1 illustrates the structural behaviour of a concrete block 10m x 8m x 13.5m subjected to load control vs displacement control loading conditions. In displacement control, Block I is subjected to AAR swelling pushing on Block II. In load control, an external force is directly applied to Block II. Block II weight W is 25 427 kN. Assuming a friction angle ϕ = 48.5°, the maximum resisting shear force, **R** that could be developed at the base of the block is 28 739 kN (given by W tanϕ). The Sliding Safety Factor (SSF) can be computed from SSF = **R** / **L**, where **L** is the applied force in load control, and the transferred force from Block I to Block II in displacement control. Figures 3.1c,d indicate that under load control, the displacement becomes unbounded as soon as **L** $>$ **R** (or SSF $<$ 1). In displacement control SSF $\cong$ 1 is maintained during sliding because **L** can not increase beyond **R**. The sliding displacement then corresponds to the imposed displacements.

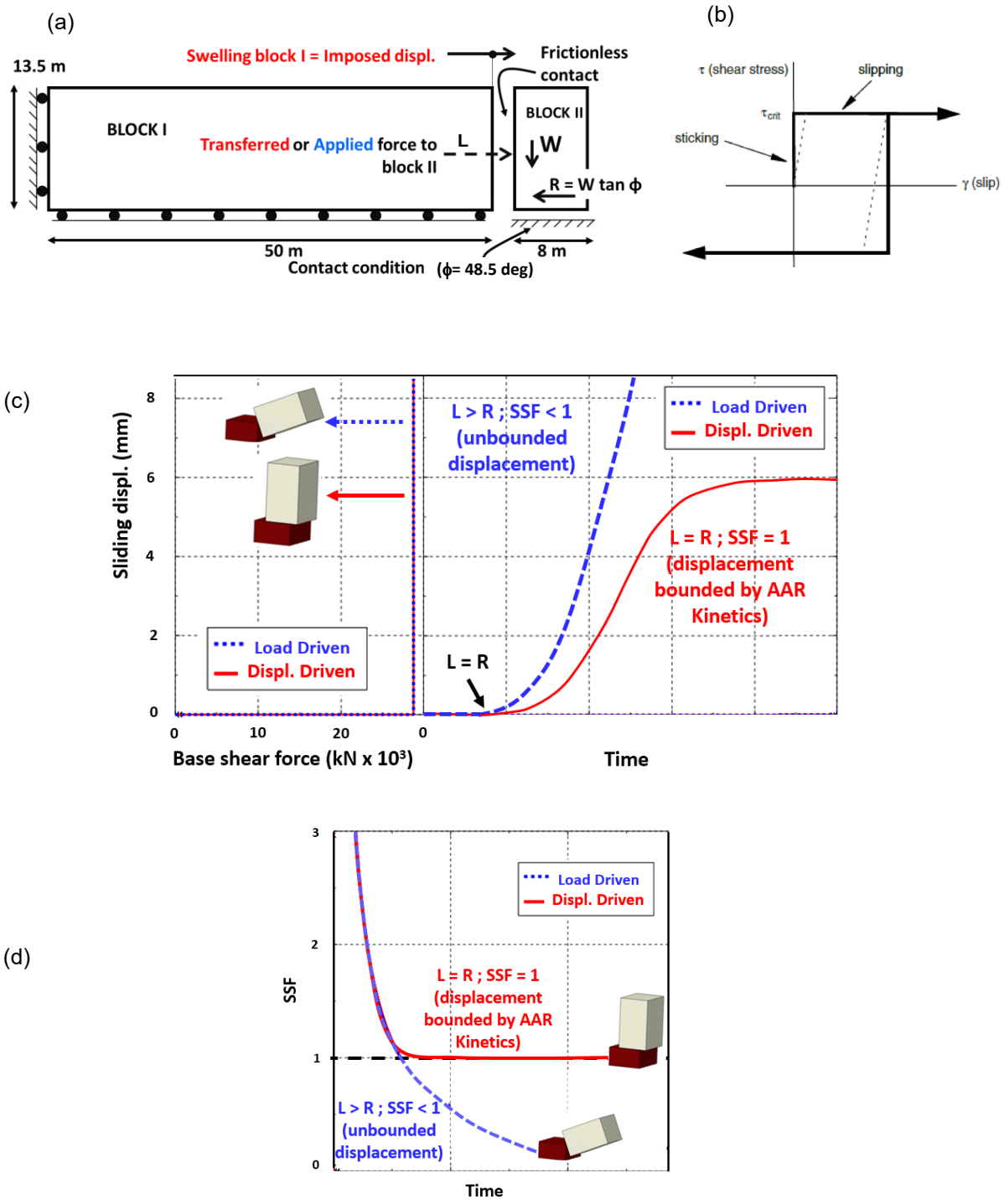

Figure 3.1 Load vs displacement control sliding response: (a) Structural model (10 m thick), (b) Stick-Slip frictional response of contact element, (c) Displacement response, (d) Sliding Safety Factor (SSF)

4. PROPOSED AAR BENCHMARK PROBLEMS

4.1 BP1 – Compressive failure

BP1 and its two variants are designed to identify the PFMs for configurations where small elements (e.g. bridge deck) are adjacent to relatively larger and stiffer elements (e.g. dam crest). No gel expansion can occur at stress intensity above 8 to 10 MPa. This compressive limiting stress for AAR kinetics is generally

a material input parameter in multi-physic models [7, 13] (parameter σ_u = 10 MPa in Table 2.1, Fig. 4.1). Therefore, theoretically no failure can occur when a single prismatic concrete element is subjected to self-restrained swelling. This case is represented by configuration BP1a in Fig. 4.1.a, where the restrained swelling direction is along X axis. However, when two adjacent elements with different cross sections are subjected to restrained swelling, the behaviour becomes different. Compressive stresses in the smaller element can exceed the AAR limiting stress because they are controlled by swelling of the larger element. Furthermore, the stress distribution is no more uniform near the junction of the two elements. Tensile stresses can develop in the perpendicular direction to the principal compressive stresses (similar to local post-tension effects). These situations are represented by configurations BP 1b and BP 1c. The only difference between these two configurations is the steel reinforcement added for BP 1c to control the tensile stresses near the junction, on the side of the larger element.

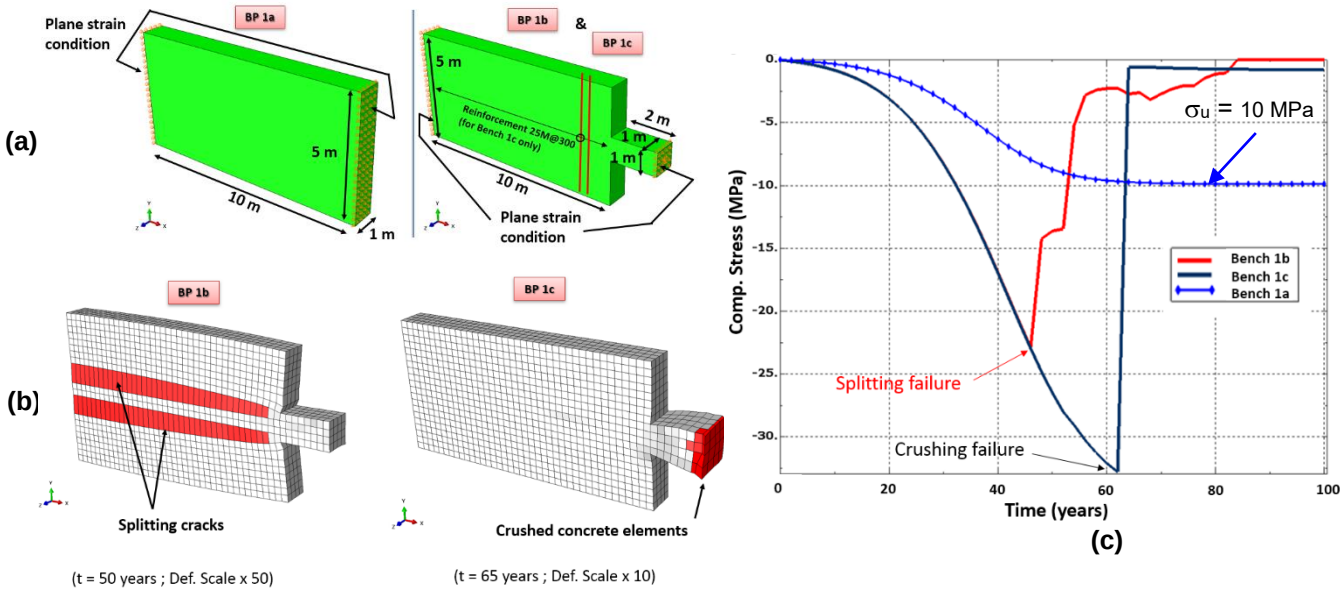

Figure 4.1 BP1 benchmarks: (a) Geometry and boundary conditions, (b) Failure modes, (c) Results of transferred compressive stress vs time

Figures 4.1.b,c present the simulation results. In Figure 4.1.c, the compressive stresses along the X axis are averaged for the last row of concrete elements subjected to plane strain condition. While no failure was recorded for BP1a, splitting and crushing failures occurred respectively for BP1b and BP1c at years 50 and 65. As expected, the compressive stresses in BP1a capped at a value of σ_u =10 MPa, which is much smaller than the compressive strength of the concrete (40 MPa), and no compressive crushing occurred. Tensile stresses developed in BP1b along Y direction, and because no reinforcement is provided, splitting cracks propagated along X direction, causing failure. The presence of rebars in BP1c allowed to control concrete cracking after its initiation. Crushing failure occurred at year 65 when the compressive stresses reached the compressive strength of concrete.

4.2 BP2 – Flexural failure

BP2 benchmark is representative of PFMs where displacement driven AAR forces are combined to load driven hydrostatic thrust. The geometry shown in Fig. 4.2.a includes a reinforced concrete pier (representative of a spillway pier) adjacent to a concrete 20 m long gravity dam. A contact condition with friction is used at their interface. Before activation of the AAR (at year 0), hydrostatic loads are applied on the upstream face of the pier. Hence, AAR thrusts coming from the dam produces bending of the pier around the Z axis, while hydrostatic loads induce bending around the X axis.

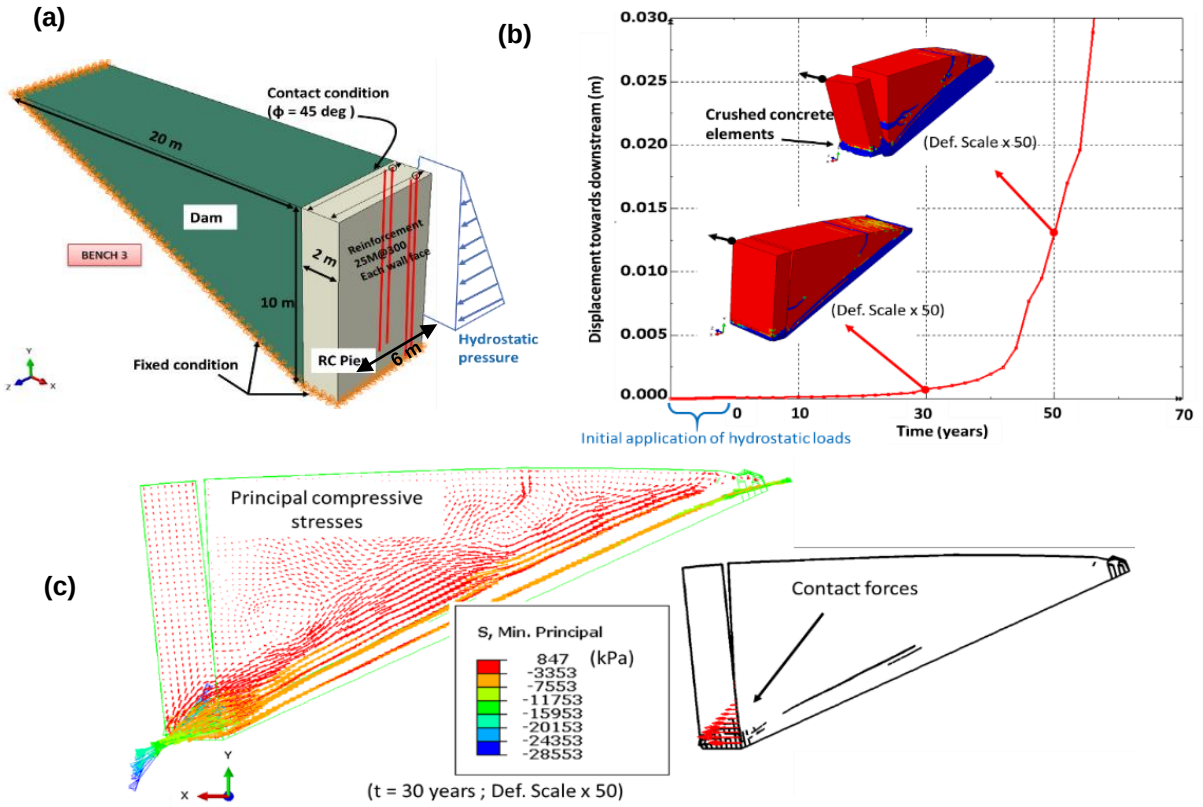

Figure 4.2 BP2 benchmark: (a) Geometry and boundary conditions, (b) Displacement results, (c) Principal compressive stresses and contact forces

Figure 4.2.b presents the displacement vs. time response of a point on top of the RC pier. The order of magnitude of the displacement when only hydrostatic loads are applied is the tenth of mm. Cracking initiates at year 30 within the dam body, but also at the base of the dam and RC pier. Orientation and position of these cracks can be explained by the contact forces acting on the pier and by the inclined AAR compressive thrust shown in Fig. 4.2.c.

Crushing at the base of the RC pier can be noticed for concrete elements. Excessive bending can be clearly seen in Fig.4.2.b at year 50. It is difficult to precisely define the failure time. Near year 55, the displacement rate becomes excessively large and flexural failure of the pier occurs. Reinforcement at the base of pier start yielding at year 20 due to bending around the Z axis. However, this did not result in failure of the pier, due to the ductile reinforcement behaviour (elasto-plastic model is used herein). The pier failure is related to crushing of concrete elements at the pier base, due to bi-axial bending. Unlike steel yielding, concrete crushing is brittle and induces a drop in the carried stresses (see also Figure 4.1.b BP 1c).

4.3 BP3 Misalignement effect

Misalignement effect along the longitudinal axis of a facility is studied in this BP. Figure 4.3 shows the geometry of BP3. It is made of two concrete blocks, representative of two adjacent components located in a corner of a hydroelectric facility. Contact condition with friction is used at the interface between the blocks. Hydrostatic pressures are applied at the beginning of the analysis on the upstream faces, prior to AAR swelling.

The contact forces between the blocks are shown in Figure 4.4. They are consequences of concrete swelling and plane strain conditions. These AAR driven forces act to push each block towards downstream, in the same direction as the load driven hydrostatic pressures.

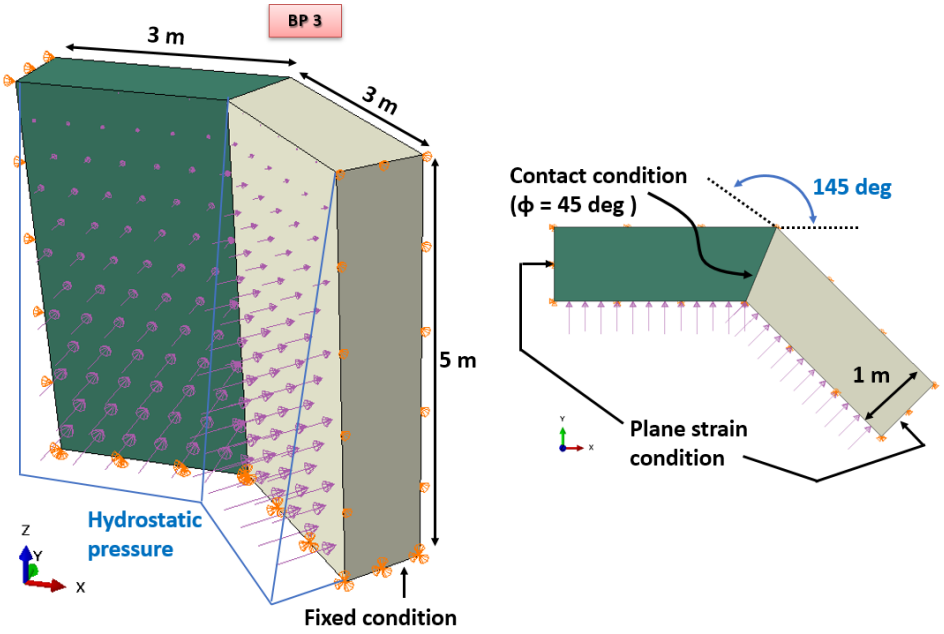

Figure 4.3 Geometry and boundary conditions for BP3

Similarly to the previous BP, Fig. 4.4 indicates that displacements induced by hydrostatic forces are of much smaller order of magnitude if compared to those induced by AAR. Around year 25, failure of the blocks occurs, due to cracking at their bases. The AAR driven contact forces result in high vertical tensile stresses that exceed the tensile strength of concrete. Like concrete crushing, the tensile cracking of concrete with no reinforcement is a local brittle failure mechanism that may result in global failure when AAR effects are combined to mechanical loads.

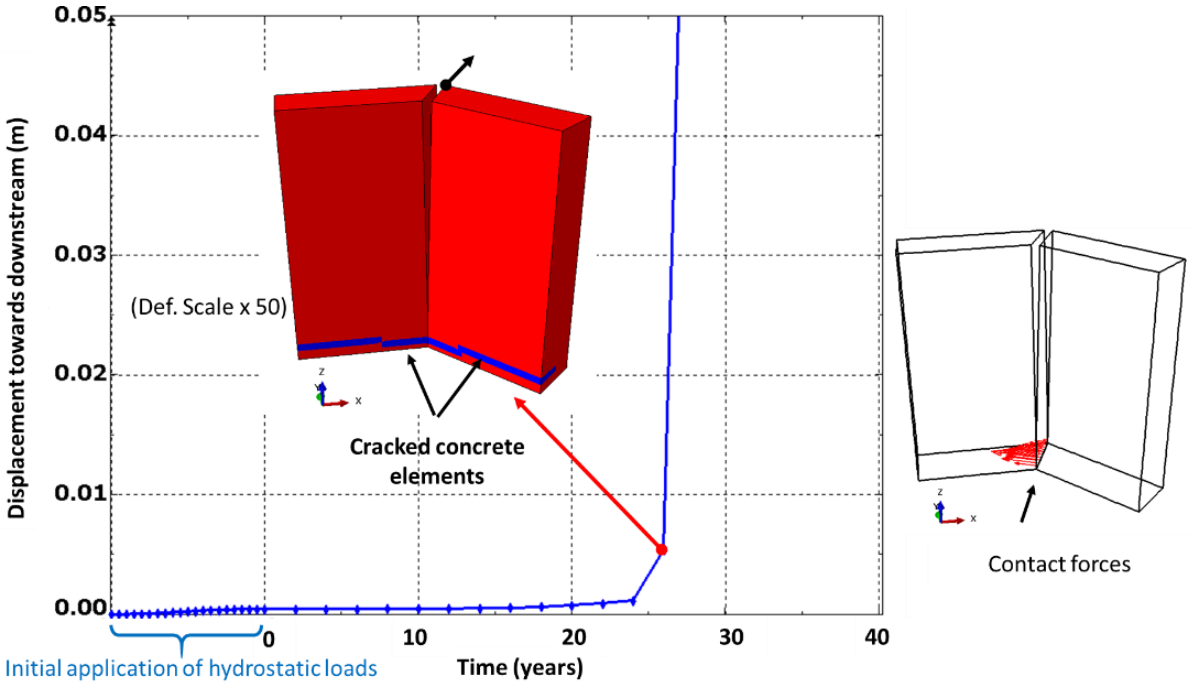

Figure 4.4 Results of BP3

5. SUMMARY AND CONCLUSIONS

The structural safety assessment and life prediction of hydroelectric facilities affected by AAR require the use of verified and validated nonlinear multi-physics finite element modelling and simulation tools. To this end, series of benchmark problems have been proposed in the specialised literature [1,6,7]. Those problems generally follow an approach of increasing complexity working from (i) the representative volume at the material scale, towards the (ii) component, and (iii) structural scale. Herein, we proposed three new simple benchmark problems at the component scale that have been developed from potential failure modes (PFMs) identified from a 100 year AAR analysis of a typical hydroelectric facility at the structural scale. They are presented to the community to verify if AAR models in use are able to capture correctly key PFMs. Herein, Saouma' s AAR FE constitutive model [7], implemented in the ABAQUS-Explicit computational platform is used in all simulations [9]. Following this study, the following conclusions are made:

(1) AAR is a displacement driven loading phenomenon that is limited to few tenth or hundred mm. It is the combination of AAR induced damage (cracking, shear strength reduction, …) with self-weight, uplift pressures, and usual, unusual or extreme loads (floods and earthquakes) that may induce failure.

(2) Compressive failure of thin concrete elements (e.g. spillway bridge deck) subjected to volumetric expansion of adjacent bulk structural components (gravity dam, powerhouse) is possible. This is despite arrest of the swelling process due to compressive stresses reaching a threshold value, σ_u. Benchmark problem no.1 has shown the crushing failure of a 1m x1m x 2m thin component in contact with a 10m x 5m x 1m large component. With this geometrical configuration, splitting tensile horizontal cracks has also been shown to develop in the large component.

(3) Benchmark problem 2 has shown the upstream – downstream flexural failure of a (spillway) pier component 2m x 6m x 10m being pushed laterally in the cross-valley direction by the swelling of an adjacent gravity dam component. The combination of AAR and hydrostatic thrusts induced concrete cracking and with the swelling progress concrete crushing.

(4) Benchmark problem 3 is typical of observed failure mode of wing gravity dams interconnected with powerhouse at an oblique angle. Two concrete walls 1 m x 3m x 5m connected at 145 degrees from each other are used for this failure mode. Failure occurs by excessive tensile cracking at the base inducing wall structural instability.

6. ACKNOWLEDGMENTS

The financial support provided by the Quebec Fund for Research on Nature and Technology (FRQNT) and the Natural Science and Engineering Research Council of Canada (NSERC) is acknowledged.

7. REFERENCES

[1] ICOLD (2019). Management of expansive chemical reactions in concrete dams & hydroelectric projects, Final Draft, Bulletin.

[2] Curtis, D.D, Feng., L., Sooch, G.S, Zheng, Fletcher, J. (2016). Practical analysis and assessment of AAR-affected dams and hydroelectric plants, 36th Annual USSD Conference Denver, Colorado, April 11-15, pp.675-694

[3] Esposito, R., Hendriks, M. A. N. (2019). Literature review of modelling approaches for ASR in concrete: a new perspective. European Journal of Environmental and Civil Engineering, 23(11), 1311-1331.

[4] Pan, J. W., Feng, Y. T., Wang, J. T., Sun, Q. C., Zhang, C. H., Owen, D. R. J. (2012). Modeling of alkali-silica reaction in concrete: a review. Frontiers of Structural and Civil Engineering, 6(1), 1-18.

[5] Oberkampf, W. L., & Roy, C. J. (2010). Verification and validation in scientific computing. Cambridge University Press.

[6] Saouma (2019). Diagnosis & Prognosis of AAR Affected Structures, State-of-the-Art Report of the RILEM Technical Committee 259-ISR (Ch 22. Benchmark Problems for AAR FEA Code Validation).

[7] Saouma, V. (2014). Numerical modeling of AAR. CRC Press.

[8] ICOLD (2011) Benchmark Workshop on Numerical Analysis of Dams - Effect of concrete swelling on the equilibrium and displacements of an arch dam, Valencia, Spain, October 20-21.

[9] Ben Ftima, M., Sadouki, H. and Brühwiler, E. (2016). Development of a computational framework for the use of nonlinear explicit approach in the assessment of concrete structures affected by alkali-aggregate reaction", Proceedings, 9th Int. Conf. on Fracture Mech. of Concrete and Concrete Struct, FRAMCOS-9, V. Saouma, J. Bolander, and E. Landis (Eds), May 22-25, Berkeley, Ca, USA, 11 pp.

[10] Larive, C. (1998). Apports combinés de l'expérimentation et de la modélisation à la compréhension de l'Alcali-Réaction et de ses effets mécaniques. Ph.D Thesis, LCPC, Paris, France, 1998.

[11] Ben Ftima, M., Yildiz, E., Abra, O. (2019). Study of concrete hydroelectric facilities affected by AAR using multi-physical simulation: Consideration of the ultimate limit state. Proceedings, International Commission on Large Dams (ICOLD) 87th Annual meeting, Ottawa, On, Canada, 11 pp.

[12] FERC (2018). Engineering guidelines for the evaluation of hydropower projects Chapter 11 - arch dams, Federal Energy Regulatory Commission, Washington, DC, USA.

[13] Léger, P., Coté, P. and Tinawi, R. (1996). Finite element analysis of concrete swelling due to alkali-aggregate reactions in dams. Computers and Structures, Vol. 60., No.4, pp. 601-611.